Commun. Theor. Phys. **57** (2012) 285–289 Vol. 57, No. 2, February 15, 2012

Modeling of Focused Acoustic Field of a Concave Multi-annular Phased Array Using Spheroidal Beam Equation*

YU Li-Li (余立立),[1,2,†] SHOU Wen-De (寿文德),[1,3] and HUI Chun (惠春)[1]

[1]Department of Biomedical Engineering, Shanghai Jiao Tong University, Shanghai 200030, China

[2]Institute of Navigation Science, Shanghai Maritime University, Shanghai 201306, China

[3]Shanghai Institute of Ultrasound in Medicine, Shanghai 200233, China

(Received February 14, 2011; revised manuscript received June 17, 2011)

Abstract *A theoretical model of focused acoustic field for a multi-annular phased array on concave spherical surface is proposed. In this model, the source boundary conditions of the spheroidal beam equation (SBE) for multi-annular phased elements are studied. Acoustic field calculated by the dynamic focusing model of SBE is compared with numerical results of the O'Neil and Khokhlov–Zabolotskaya–Kuznetsov (KZK) model, respectively. Axial dynamic focusing and the harmonic effects are presented. The results demonstrate that the dynamic focusing model of SBE is good valid for a concave multi-annular phased array with a large aperture angle in the linear or nonlinear field.*

PACS numbers: 43.25.+y, 43.80.+p
Key words: axial dynamic focusing, SBE, acoustic field, multi-annular phased array

1 Introduction

High intensity focused ultrasound (HIFU) is a promising technique as a noninvasive local treatment approach, which can induce coagulation necrosis in targeted tissues for a very short time, while the skin and surrounding tissues are slightly damaged.[1−2] Three different techniques — geometrical, acoustic, and electronic phased focusing — are often available for efficient focusing. For superficial tumors under the scarfskin, such as cervical lesions, geometrical self-focusing with a single element of a concave spherical transducer is used in focused ultrasound surgery. However, due to different locations and sizes of actual lesions, the focus position must be adjusted more accurately within a certain range. Thus, changing focus positions within a short focal length by mechanical movement is difficult for a single self-focusing element. The concave spherical transducer is axial symmetric and can only focus on the central axis; hence, the concave spherical surface is often divided into multiple rings for phased focusing to shift focus positions and achieve axial dynamic focusing.

Previous studies on multi-annular phased arrays on concave spherical transducers were mainly conducted using the O'Neil model.[3−5] However, the O'Neil solution is more suitable for linear acoustic fields under a relatively weak curvature of source and sufficiently high frequency. Although numerical investigations by Coulouvrat[6] and experiments by Mair *et al.*[7] indicated that the O'Neil's model is well applicable for large aperture angles (up to 60°), it is not fit for high frequencies when the value of ka is within the range of 10 to 50, where k is the wave number and a is the half-aperture. To describe the combined effects of diffraction, absorption and nonlinearity in focused ultrasound beams, the Khokhlov–Zabolotskaya–Kuznetsov (KZK) equation is extensively used as a model either in time or frequency domain for finite amplitude sound propagation.[8−11] However, the KZK model is more suitable for a weak focused ultrasound beam because that it derived under the paraxial approximation and the upper limit of the applicability is about 16° for the half aperture angle.[12] The spheroidal beam equation (SBE) proposed by Kamakura *et al.*[13] use the oblate spheroidal coordinate system for theoretical prediction on focused ultrasound beams with a circular aperture; the upper limit of the half aperture angle is up to 40°. Moreover, SBE can be easily extended to the analysis of nonlinear harmonic generation with high frequencies in finite amplitude sound beams.[14−15] However, SBE is generally used to describe sound propagation for geometrical self-focusing transducers with fixed focal lengths.[16−17] Currently, there are few reported results referring to SBE application in multi-annular phased focusing on a concave spherical surface.

In this letter, we study source boundary conditions for a multi-annular phased array on a concave spherical surface using SBE. A transducer array with a large aperture angle and multi-annular elements is used to validate the

*Supported by the National Natural Science Foundation of China under Grant Nos. 39970209 and 30772072
†E-mail: liliyu@sjtu.edu.cn

feasibility of using the dynamic focusing model of SBE in solving the acoustic field of a phased array on a concave spherical surface. The linear and nonlinear field calculated by the dynamic focusing model of SBE is compared with that of the O'Neil and KZK model, respectively. Axial dynamic focusing is discussed. Moreover fundamental and harmonic sound propagation is theoretically investigated.

2 Theory and Methods

2.1 *Spheroidal Beam Equation*

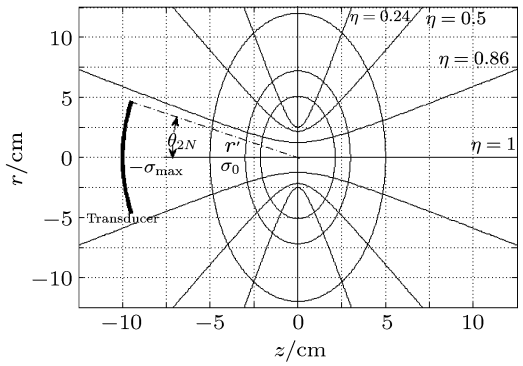

Fig. 1 Oblate spheroidal coordinate system.

To explain sound propagation with a large aperture angle, we apply SBE in an oblate spheroidal coordinate system (Fig. 1).[13−14] The focused ultrasound field is divided into two regions, i.e., $\sigma < \sigma_0$ and $\sigma \geq \sigma_0$, where σ_0 denotes a specific transition location. The former division near the source is a spherical wave region, and the latter division near the focus is a plane wave region. The SBE model to describe the spheroidal and planar waves in two regions are expressed as follows respectively:

$$\begin{aligned}&\frac{\partial^2\bar{p}}{\partial\tau_s\partial\sigma}+\frac{1}{2}\frac{\sin 2\theta}{\sigma(1+\sigma^2)}\frac{\partial^2\bar{p}}{\partial\tau_s\partial\theta}\\&+\frac{\varepsilon\sqrt{\sigma^2+\sin^2\theta}}{\sigma(1+\sigma^2)}\Big(\frac{\partial^2\bar{p}}{\partial\theta^2}+\cot\theta\frac{\partial\bar{p}}{\partial\theta}\Big)+\frac{E}{\sigma}\frac{\partial\bar{p}}{\partial\tau_s}\\=&-\frac{\sqrt{\sigma^2+\sin^2\theta}}{\sigma}\Big(\alpha b\frac{\partial^3\bar{p}}{\partial\tau_s^3}+\frac{b}{2l_D}\frac{\partial^2\bar{p}^2}{\partial\tau_s^2}\Big)E\\&(\sigma<\sigma_0<0),\end{aligned}\tag{1}$$

$$\begin{aligned}&\frac{\partial^2\bar{p}}{\partial\tau_p\partial\sigma}-\frac{\sigma}{1+\sigma^2}\sin\theta\frac{\partial^2\bar{p}}{\partial\tau_p\partial\theta}\\&-\frac{\varepsilon(2-\cos\theta)}{1+\sigma^2}\Big(\frac{\partial^2\bar{p}}{\partial\theta^2}+\cot\theta\frac{\partial\bar{p}}{\partial\theta}\Big)\\=&\Big(\alpha b\frac{\partial^3\bar{p}}{\partial\tau_p^3}+\frac{b}{2l_D}\frac{\partial^2\bar{p}^2}{\partial\tau_p^2}\Big)E\quad(\sigma\geq\sigma_0,\sigma_0<0),\end{aligned}\tag{2}$$

where the variables (σ,η) in the oblate spheroidal coordinate are related to the cylindrical coordinate (r,z) through the relationships of $r=b\sqrt{(1+\sigma^2)(1-\eta^2)}$ and $z=b\sigma\eta$, in which b is the half inter-focal length. The angle variable θ is related to η as $\eta=\cos\theta$. The coefficient ε is set at $1/2kb$ and E is a function of σ and θ; τ_s is the spherically retarded time near the source; τ_p is the retarded time for planar waves near the focus; $\bar{p}=p/p_0$ is the normalized sound pressure with p_0 as the initial amplitude of sound pressure on the surface of the source; α is the sound attenuation coefficient; l_D is shock formation distance for a planar wave, which is related to the nonlinear coefficient β of the medium.[14−15] If $\beta=0$, the SBE model can be used to predict linear fields.

In the frequency domain, the solutions of Eqs. (1) and (2) are represented by the following Fourier series expansions, respectively,

$$\bar{p}=\begin{cases}\sum\limits_{n=1}^{\infty}[g_n^{(s)}\sin(n\tau_s)+h_n^{(s)}\cos(n\tau_s)],\\(\sigma<\sigma_0<0),\\\sum\limits_{n=1}^{\infty}[g_n^{(p)}\sin(n\tau_p)+h_n^{(p)}\cos(n\tau_p)],\\(\sigma\geq\sigma_0,\sigma_0<0),\end{cases}\tag{3}$$

where $g_n^{(s)}$, $h_n^{(s)}$, $g_n^{(p)}$, and $h_n^{(p)}$are amplitude components of the n-th harmonic and are functions of the spatial variables σ and θ. Details of the spheroidal beam equation (SBE) are described in Ref. [13].

2.2 *Dynamic Focusing Model*

Figure 2 illustrates the configuration of a focused sound source, which consists of several concentric rings placed on a concave spherical surface and rings are numbered as 1, 2, ..., and N along z-axis. Point F is the desired focus, point o is located at the bottom of the source, and point O is the geometrical center. The notation l is the focal length, r' is the radius of the curvature, θ_{2N} is the half-aperture angle, a is the half-aperture, d is the distance from the i-th ring ($i\leq N$) to focus F, w and h is the arc-width of ring and the arc-space between adjacent rings on the surface of transducer respectively. To realize a focusing system with a multi-annular phased array in which all waves from each ring arrive at focus F in the phase, a relative phase ϕ_i for the i-th ring is applied. Consequently, boundary conditions at the source in the SBE system yield the following relation:

$$\begin{aligned}&\bar{p}|_{\sigma=-\sigma_{\max}}\\=&\begin{cases}U(\theta)\sin(\tau_s+\phi_i), & (\theta_{2i-1}\leq\theta\leq\theta_{2i}),\\0, & (\text{others}),\end{cases}\end{aligned}\tag{4}$$

where the outer and inner half-aperture angles of the i-th ring are indicated by θ_{2i} and θ_{2i-1} , respectively. Additionally, $U(\theta)$ is the pressure distribution function on the surface of the source; it becomes $U(\theta)=1$ when pressure is uniformly distributed. The relative phase of the i-th ring can be written as $\phi_i=2\pi(d-l)/\lambda$, where λ is the wavelength. The distance from the i-th ring to focus F can then be written as

$$d = \begin{cases} \sqrt{r'^2 + (r'-l)^2 - 2r'(r'-l)\cos\theta_m}, & (l \le r'), \\ \sqrt{r'^2 + (l-r')^2 - 2r'(l-r')\cos(180^\circ - \theta_m)}, & (l > r'), \end{cases} \tag{5}$$

where the center half-aperture angle of the i-th ring can be expressed as $\theta_m = (\theta_{2i} + \theta_{2i-1})/2$. Focus F located at the left of point O, i.e., $l \le r'$, is shown in Fig. 2(a); $l > r'$ is shown in Fig. 2(b). Thus, the initial values of $g_1^{(s)}$ and $h_1^{(s)}$ at $\sigma = -\sigma_{\max}$ are given through the boundary condition of Eq. (4):

$$g_1^{(s)} = \begin{cases} \cos\phi_i, & (\theta_{2i-1} \le \theta \le \theta_{2i}), \\ 0, & (\text{others}), \end{cases}$$
$$h_1^{(s)} = \begin{cases} \sin\phi_i, (\theta_{2i-1} \le \theta \le \theta_{2i}), \\ 0, (\text{others}). \end{cases} \tag{6}$$

Then, the fundamental pressure amplitudes at $\sigma = -\sigma_{\max}$ are obtained by $\sqrt{g_1^{(s)^2} + h_1^{(s)^2}}$.

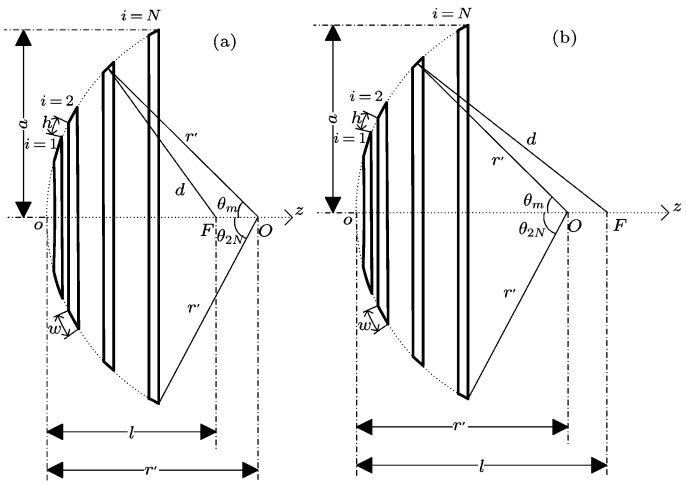

Fig. 2 Concave multi-annular focusing source geometry. (a) $l \le r'$, (b) $l > r'$.

3 Numerical Examples

To examine the validity of SBE for a phased focusing source with a concave spherical transducer, firstly, the axial dynamic focusing is carried out for three different of setting points (e.g., −2.5 cm, 0 cm, and 2.5 cm) along z-axis with $f = 1$ MHz, $p_0 = 450$ Kpa, $r' = 10$ cm, $\theta_{2N} = 30^\circ$ and a continuous variable phase (i.e., N is enough much and h are rather minute.) In addition, degassed water, with sound velocity $c_0 = 1500$ m/s, density $\rho_0 = 1000$ kg/m^3, nonlinear coefficient $\beta = 0$, and attenuation coefficient $\alpha = 0.0253$ Np/m at 1 MHz with frequency dependence f^2, is used as the propagation medium in the simulation. Since it is not easy to solve the SBE equation analytically, numerical computation is performed by means of an implicit backward finite difference method. For ensuring reasonable accuracy, we establish 600 grid points from 0 to $\pi/2$ on the θ axis, and thus the step size of θ is 2.618×10^{-3} rad. The transition location is numerically determined to be a reasonable choice for $\sigma_0 = -1.0$.[14,18]

An interesting comparison is shown in Fig. 3 for the linear SBE and O'Neil solutions. It can be seen that the difference between the solutions is discernible when the setting focal length l is larger than the radius of curvature r', but both models are basically in agreement in the focal region. Moreover, previous experiments[5] validated effectiveness of O'Neil model on concave multi-annular phased arrays. Consequently, the dynamic focusing model of linear SBE is also good valid for a multi-annular phased array on a concave spherical surface with a large aperture angle in the linear field.

Then, we set $\theta_{2N} = 15^\circ$ and $\beta = 3.5$ while other parameters remain unchanged, and make a comparison with result from the KZK model. The axial distribution of acoustic fields calculated using nonlinear SBE and the KZK model within the setting range of focus position for the fundamental, second and third harmonics is shown in Figs. 4, 5, and 6, respectively. It can be found that the pressure amplitude from nonlinear SBE is slightly smaller than that from KZK model with different setting positions of focus z_F and the maximum deviation is less than 3%, but both models are in good agreement in the focal region for the fundamental, second and third harmonics. Therefore, the nonlinear effect of the dynamic focusing model of SBE is almost consistent with KZK model for a multi-annular phased array on a weakly focusing concave spherical surface. In addition, the higher the harmonics, the shorter is the −3 dB axial length of the focal region. This suggests that the focused energy is primarily directed to the focus and the higher harmonics focus better than the fundamental, which is beneficial in improving nonlinear imaging qualities for monitoring treatment effects. In this case, a relative harmonic peak pressure amplitude is defined as $g_{hn} = p_n/p_1$, where p_1 is the fundamental peak pressure and p_n is the n-th harmonic peak pressure. For different setting positions of focus z_F (e.g., −2.5 cm, 0 cm, and 2.5 cm), the g_{h2} values are 47.3%, 50.2%, and 51.4%, respectively. Correspondingly, these values are 29.8%, 33.3%, and 34.7% for the third harmonic. The results show that with increasing focal length l, the nonlinear effect becomes stronger.

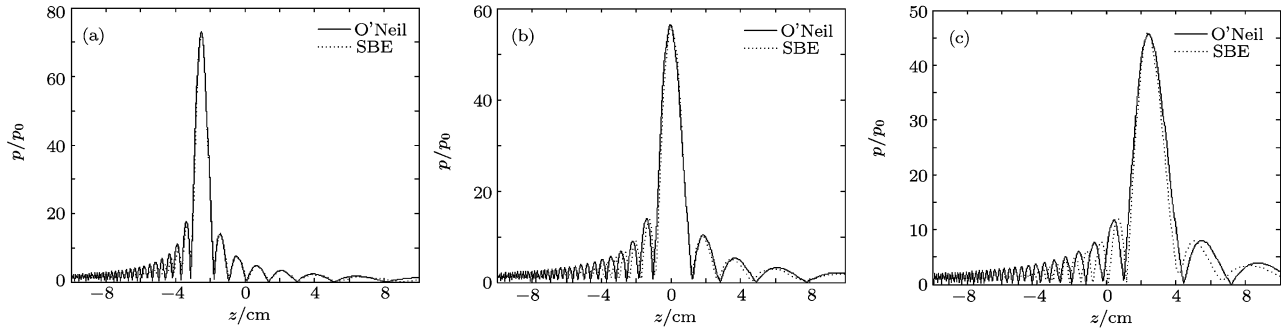

Fig. 3 Comparison of normalized axial pressure amplitude between the linear SBE model (dotted curves) and O'Neil (solid curves) model for different setting positions of focus z_F with $f = 1$ MHz, $r' = 10$ cm, and $\theta_{2N} = 30°$. (a) $z_F = -2.5$ cm, (b) $z_F = 0$ cm, (c) $z_F = 2.5$ cm.

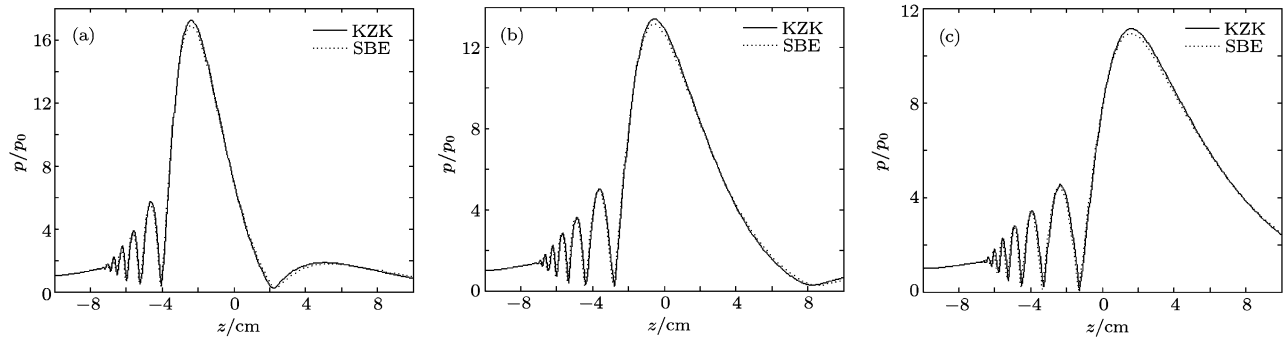

Fig. 4 Comparison of normalized axial pressure amplitude (fundamental) between the nonlinear SBE model (dotted curves) and KZK (solid curves) model for different setting positions of focus z_F with $f = 1$ MHz, $r' = 10$ cm and $\theta_{2N} = 15°$. (a) $z_F = -2.5$ cm, (b) $z_F = 0$ cm, (c) $z_F = 2.5$ cm.

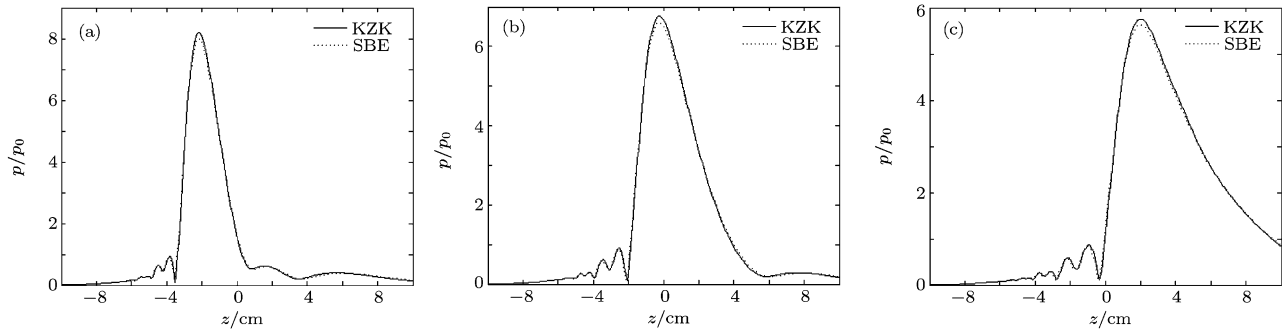

Fig. 5 Comparison of normalized axial pressure amplitude (second-harmonic) between the nonlinear SBE model (dotted curves) and KZK (solid curves) model for different setting positions of focus z_F with $f = 1$ MHz, $r' = 10$ cm and $\theta_{2N} = 15°$. (a) $z_F = -2.5$ cm, (b) $z_F = 0$ cm, (c) $z_F = 2.5$ cm.

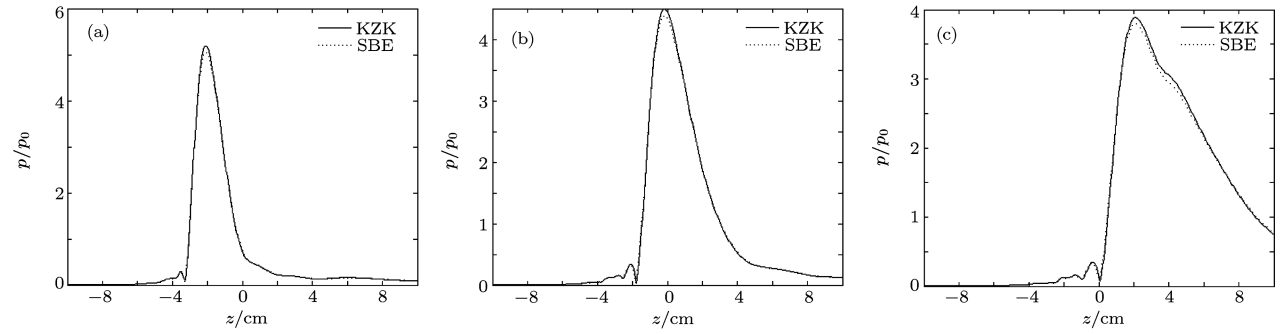

Fig. 6 Comparison of normalized axial pressure amplitude (third-harmonic) between the nonlinear SBE model (dotted curves) and KZK (solid curves) model for different setting positions of focus z_F with $f = 1$ MHz, $r' = 10$ cm and $\theta_{2N} = 15°$. (a) $z_F = -2.5$ cm, (b) $z_F = 0$ cm, (c) $z_F = 2.5$ cm.

Finally, whatever the model with self-focusing on a concave spherical surface, there is slight deviation in focus positions when the setting position of the focus is near the geometrical center. Except for the geometrical focus, the deviation increases as the setting position goes farther from sound source along z-axis. Particularly, when the setting focal length l is larger than the radius of curvature r', the deviation in focus positions is apparently greater and the -3dB axial length of the focal region is longer, indicating poor focusing properties.

4 Conclusion

In conclusion, this study proposed source boundary conditions using SBE for a multi-annular phased array on a concave spherical transducer. The numerical computations and previous experiments[5] validate the effectiveness of linear SBE in solving for the linear acoustic field of a multi-annular phased array on a concave spherical surface. The pilot study of the nonlinear field by the SBE model is also implemented, numerical results of which are in good agreement with that of the KZK model. The simulations show that axial dynamic focusing is feasible but the setting range of focus is limited. In addition, with increasing focal length, the nonlinear effect becomes stronger.

Compared with the O'Neil and KZK model, the dynamic focusing model of SBE lays a theoretical basis for the study of axial dynamic focusing and nonlinear harmonic effects under high frequencies and large aperture angles. To validate the effectiveness of nonlinear effect of the present model, appropriate experiments should be conducted in our further studies.

Acknowledgments

The authors thank Prof. Tomoo Kamakura, the university of Electro-Communication, Japan, for his useful help in solving the SBE programming. The authors are also grateful to the editors and the reviewers for their valuable comments.

References

[1] J. Bohannon, Science **321** (2008) 338.
[2] G.R. Ter Haar, Phys. Med. Biol. **34** (1989) 1743.
[3] H.T. O'Neil, J. Acoust. Soc. Am. **21** (1949) 516.
[4] M. Arditi, F.S. Foster, and J.W. Hunt, Ultrasonic Imaging **3** (1981) 37.
[5] T. Fjield, X.B. Fan, and K. Hynynen, J. Acoust. Soc. Am. **100** (1996) 1220.
[6] F. Coulouvrat, J. Acoust. Soc. Am. **94** (1993) 1663.
[7] H.D. Mair and D.A. Hutchens, *Proc. 12th Int. Congress on Acoustics*, Plenum, New York (1987) 619.
[8] J. Naze Tjϕtta and S. Tjϕtta, Acta Acustica **1** (1993) 69.
[9] X. Yang and R.O. Cleveland, J. Acoust. Soc. Am. **117** (2005) 113.
[10] M.H. Liu, J.L. Li, C. Yin, X.F. Gong, D. Zhang, and H.H. Xue, Phys. Lett. A **362** (2006) 50.
[11] R. Williams, E. Cherin, T.Y.J. Lam, J. Tavakkoli, R.J. Zemp, and F.S. Foster, Phys. Med. Biol. **51** (2006) 5809.
[12] J. Naze Tjϕtta, S. Tjϕtta, and E.H. Vefring, J. Acoust. Soc. Am. **89** (1991) 1017.
[13] T. Kamakura, T. Ishiwata, and K. Matsuda, J. Acoust. Soc. Am. **107** (2000) 3035.
[14] T.B. Fan, Z.B. Liu, Z. Zhang, D. Zhang, and X.F. Gong, Chin. Phys. Lett. **26** (2009) 084302
[15] M.H. Liu, D. Zhang, and X.F. Gong, Chin. Phys. Lett. **24** (2007) 2267.
[16] S.Y. Qian, T. Kamakura, and M. Akiyama, Ultrasonics **44** (2006) 271.
[17] R.M. Xia, W.D. Shou, G.P. Chen, and H.Z. Wang, Chin. Phys. Lett. **19** (2002) 355.
[18] R.M. Xia, W.D. Shou, G.P. Chen, and M.D. Zhang, J. Comput. Acoust. **11** (2003) 47.